Performance Prediction and Testing of Cryogenic Liquefied Gas Reaction Turbines

Sarah Alison-Youel, Research and Development Engineer
Ebara International Corporation
Sparks, NV

AIChE Spring Meeting, April 2009
9th Topical Conference on Natural Gas Utilization
Tampa, Florida, April 26-30, 2009

Abstract

A new general performance equation has been previously presented for fixed geometry hydraulic reaction turbines and it has been shown to have a more accurate representation of liquefied hydrocarbon gas reaction turbine performance. This paper develops further equations relating the affinity laws and the conservation of energy and momentum laws to predict efficiency curves and the best efficiency point.

Due to the nature of the cryogenic environment in which liquefied gas reaction turbines operate, acquiring dependable test data presents a unique set of conditions. This paper also reviews the current testing techniques developed and used by Ebara International Corporation (EIC).

The presented equations are the most general, as well as, most accurate tools for turbine performance prediction. Actual test data from an EIC liquefied gas reaction turbine is used to investigate the presented equations.

Introduction

Lobanoff et al (1992) presented the affinity law relationships for pumps and suggested that they also apply to hydraulic reaction turbines. In 2008, Alison-Youel developed a partial model for liquefied gas reaction turbine performance. Also in 2008, Finley developed a method for predicting liquefied gas reaction turbine performance using the no-load and locked-rotor characteristics. This paper attempts to complete turbine performance modeling and prediction by investigating the available hydraulic power, developing a new general shaft power equation, and subsequent efficiency equation. These new developments are also investigated in order to predict the best efficiency point (BEP).

In order to achieve this, two very important assumptions are made. First, the turbine is of constant geometry; therefore, radius, cross-sectional area, and angles are fixed. Second, the working fluid is in-compressible; therefore, the fluid density is constant. Another key aspect to be addressed relates to the specific design of a submerged

generator hydraulic liquefied gas reaction turbine and the testing of these types of machines.

Nomenclature

SG	Specific Gravity
H	Head
Q	Volume Flow Rate
N	Rotational Speed
$\alpha, \beta, \gamma, \lambda, \delta$	General Performance Equation and No-Load Constants
P_{hy}	Available Hydraulic Power
b	Unit Conversion Constant for Hydraulic Power Equation
M_{rot}	Rotational Momentum
v	Velocity
R, r	Outer and Inner Hydraulic Radius
P_{shaft}	Shaft Power
m, n	Summation Indices
a, b	Indices Representing Distinct Operating Points
k	Shaft Power Constant
ξ	BEP Constant

Testing Cryogenic Hydraulic Reaction Turbines

The inherent nature of a cryogenic environment coupled with the integrated turbine hydraulics and submerged generator design creates a special set of circumstances that drive the testing and data acquisition of liquefied gas reaction turbines.

Figure 1 is a simplified solid model of the most recent EIC single stage liquefied gas reaction turbine. Due to the submerged generator design it is not possible to separate the hydraulic performance from the generator performance without major design alteration. Therefore, the overall turbine efficiency is inclusive of the generator and the hydraulic efficiencies.

During testing, multiple pieces of data are measured and recorded. After testing is complete the raw data recorded during testing is then reduced into understandable and useable information. Table 1 tabulates the instrumentation used for the data collected and the subsequent units.

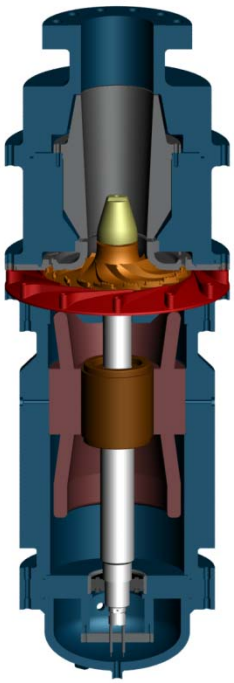

Fig. 1: Turbine Solid Model

Table 1: Recorded Test Data

Desired Data	Instrumentation	Raw Data Units	Reduced Data Units
Flow Rate	Venturi Flow Meter	inches of H_20	m^3/s or m^3/hr
Turbine Differential Pressure	Differential Pressure Transmitter	PSI	Bar
Vessel Inlet & Outlet Pressure	Pressure Transmitter (Bordon Tube)	PSIG	Barg
Speed	Eddy Probe and Target	Voltage pulse	RPS or RPM
Turbine Inlet & Outlet Temperature	1000 Ω RTD Probe	^oC	^oF
Vessel Inlet and Outlet Temperature	1000 Ω RTD Probe	^oC	^oF
Generator Output	Power Analyzer	kW, Hz, V, A	kW, Hz, V, A
Drive Output	Power Analyzer	kW, Hz, V, A	kW, Hz, V, A

Prior to turbine start-up the specific gravity (SG) of the fluid is measured and the relationship $SG = m \cdot T + c$ is calculated. Using this linear relationship, the temperature measurements are used to calculate the SG at each recorded test point. Following testing, the recorded data is used to calculate the flow, head, power output, and efficiency of the machine.

Data collected in this manner for an EIC turbine is utilized for demonstration and analysis in the following sections. The model used is LX14-07, with a nominal flow 1400 m3/hr, nominal head 700 m, and is designed to expand liquid natural gas (LNG). Test data was collected and reduced for turbine performance under the no-load condition and at the following speeds: 2400 RPM; 3110 RPM; 4000RPM.

General Performance Equation & No-Load Speed Curves

Using the above mentioned test data and the following General Performance Equation (Alison-Youel, 2008),

$$H = \alpha Q^2 + \beta N^2 + \gamma QN \tag{1a}$$

A least square error fit was applied to the full set of test data to find the constants, α, β, and γ, yielding the following surface fit equation,

$$H = 4174.85Q^2 + 0.115032N^2 - 9.42532QN \tag{1b}$$

This equation provides a three-dimensional surface fit for the performance of the turbine at multiple speeds and flow rates. Another important aspect to the performance of a turbine is when the machine is spinning, but the generator is not applying a torque. This

is known as the no-load curve. Finley (2008) provides the following relationships between, flow, rotational speed, and head under the no-load condition,

$$Q = \lambda N \tag{2a}$$

$$H = \delta Q^2 \tag{3a}$$

Again, a least square error surface fit was performed, using only the no-load condition data to produce the following relationships,

$$Q = 0.002596N \tag{2b}$$

$$H = 17610.1Q^2 \tag{3b}$$

Figure 2 is a two-dimensional plot of the actual test data and the resulting surface fit curves for the no-load condition and three speeds.

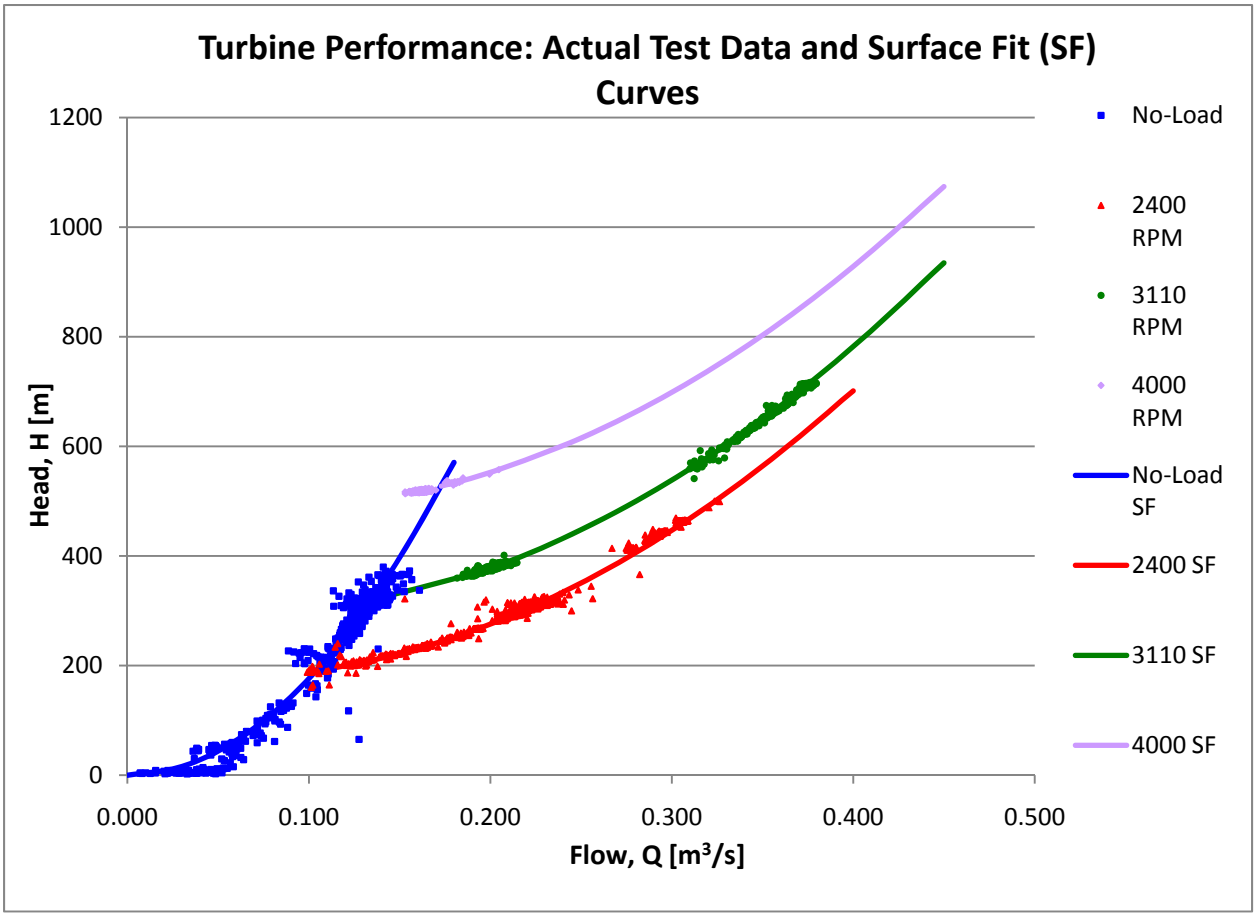

Fig. 2: Actual Test Data and Surface Fit Curves

Available Hydraulic Power

As Lobanoff et al (1992) states, the hydraulic power output of turbomachinery is proportional to the product of volume flow rate and head. Following the above calculations and surface fit equations, it follows that the available hydraulic power is,

$$P_{hy} = bQ(\alpha Q^2 + \beta N^2 + \gamma QN) \tag{4}$$

Where, the constant b is a unit conversion constant which includes the fluid density and gravity. As was previously mentioned, it is assumed that the operating fluid is incompressible; therefore, the density is a constant value.

Shaft Power

This section will develop the most general equation for shaft power that follows the conservation of energy and is based upon the conservation of momentum and the affinity law relationships.

Shaft power is a product of the rotational speed and torque experienced by the shaft. Test data provides rotational speed values leaving a relationship for torque based on test data to be found. The conservation of momentum principal applied to rotating machinery states that, torque is equal to the change in rotational momentum. The change in rotational momentum is a result of the change in mass flow, radius, and velocity. In the case of constant geometry, as is assumed in this paper, the radius, fluid flow passage area, and angels are fixed. Furthermore, due to conservation of mass, the mass flow rate is also constant. Hence, the change in rotational momentum is directly proportional to the change in velocity,

$$\Delta M_{Rot} \propto \Delta v \tag{5}$$

The change in velocity is a function of volume flow rate and rotational speed and can be developed into a general Taylor polynomial (Courant, 2000),

$$\Delta v = f(Q, N) = \sum_{m,n=0}^{\infty} C Q^m N^n \tag{6}$$

Applying this new polynomial for velocity (Eq. 6) to rotational momentum and substituting volume flow rate for mass flow rate, the following relationship is developed,

$$\Delta M_{rot} = Q\left[R \sum_{m,n=0}^{\infty} C_{1_{m,n}} Q^m N^n - r \sum_{m,n=0}^{\infty} C_{2_{m,n}} Q^m N^n\right] \tag{7}$$

Combining and simplifying, Eq. 7 becomes,

$$\Delta M_{rot} = Q \sum_{m,n=0}^{\infty} C_{m,n} Q^m N^n \tag{8}$$

The shaft power is then,

$$P_{shaft} = NQ \sum_{m,n=0}^{\infty} C_{m,n} Q^m N^n \tag{9}$$

The affinity law relationships for two distinct operating points (Lobanoff, 1992) are now utilized to solve Eq. 9 into a meaningful equation. The following are relationships from the affinity laws,

$$\frac{Q_a}{Q_b} = \frac{N_a}{N_b} = x \tag{10}$$

$$\frac{H_a}{H_b} = \frac{Q_a^2}{Q_b^2} = \frac{N_a^2}{N_a^2} = y = x^2 \tag{11}$$

As was mentioned above, hydraulic power is the product of head and flow. Applying this to the affinity law relationships,

$$\frac{P_a}{P_b} = \frac{H_a Q_a}{H_b Q_b} = xy = x^3 \tag{12}$$

Applying Eq. 10, 11, and 12 to 9 for distinct operating point a,

$$P_{shaft_a} = N_a Q_a \sum_{m,n=0}^{\infty} C_{m,n} Q_a^m N_a^n = \sum_{m,n=0}^{\infty} C_{m,n} Q_a^{m+1} N_a^{n+1} \tag{13}$$

Now applying Eq. 10, 11, and 12 to 13, a relationship for the power at each distinct operating point (a and b) is found,

$$x^3 P_{shaft_b} = \sum_{m,n=0}^{\infty} C_{m,n} X^{m+1} Q_a^{m+1} X^{n+1} N_a^{n+1} = \sum_{m,n=0}^{\infty} C_{m,n} X^{m+n+2} Q_a^{m+1} N_a^{n+1} \tag{14}$$

Equation 14 is only a true statement if $x^3 = x^{m+n+2}$ is true; more simply if, $m + n = 1$. There are only two cases where this is possible (Table 2).

Table 2: Possible Cases for m and n

m	n
0	1
1	0

Applying the values for the indices in Table 2 to Eq. 14, a functional relationship for shaft power is found,

$$P_{shaft} = NQ(C_{1,0} + C_{0,1} N) \tag{15}$$

However, at this point the constants $C_{1,0}$ and $C_{0,1}$ are not known, but the known relationships presented above for the no-load condition are applicable and reduce the number of unknown constants. Under the no-load condition torque is zero; therefore, the power is also zero. In addition, flow and rotational speed are related by the constant λ (Eq. 2a). Using this information, $C_{0,1}$ is solved for in terms of $C_{1,0}$, and λ. Putting it all together and simplifying,

$$P_{shaft} = kNQ(Q - \lambda N) \tag{16}$$

The Shaft Power Constant, k, at this point is still an unknown value. However, the value of k can be found using test data and will be further investigated in the following sections. Equation 16 is the most general equation that incorporates conservation of energy, conservation of momentum, and the affinity law relationships. More importantly, Eq. 16 was derived from a general polynomial to arrive at a specific relationship for shaft power, which supports the empirically presented equation for shaft power by Kimmel in 1997.

Power Curves & Efficiency

As mentioned above, due to the design and nature of testing cryogenic turbines the performance of the hydraulics and generator are fully integrated, and therefore, the measurable power output incorporates the efficiencies and losses in both the hydraulics and the generator. Therefore, the power output data measured during testing (in kW) is equal to the shaft power (Eq. 16). The full set of test data was again employed in a least square error fit to deduce the value of the shaft power constant, k. The resulting surface fit for the shaft power curves is shown in a two-dimensional plot (Fig. 3).

Following the deduction of the value for the Shaft Power Constant, the efficiency of the machine was analyzed. Turbine efficiency is the ratio of actual power output to available power input (Cengel, 2002). Applying the above developed equations (Eq. 4 and Eq.16) and applying them to this definition, the following relationship for efficiency, η, is found,

$$\eta = \frac{kN(Q-\lambda N)}{d(\alpha Q^2+\beta N^2+\gamma QN)} \tag{17}$$

This relationship was applied to the tested data and the results plotted (Fig. 4).

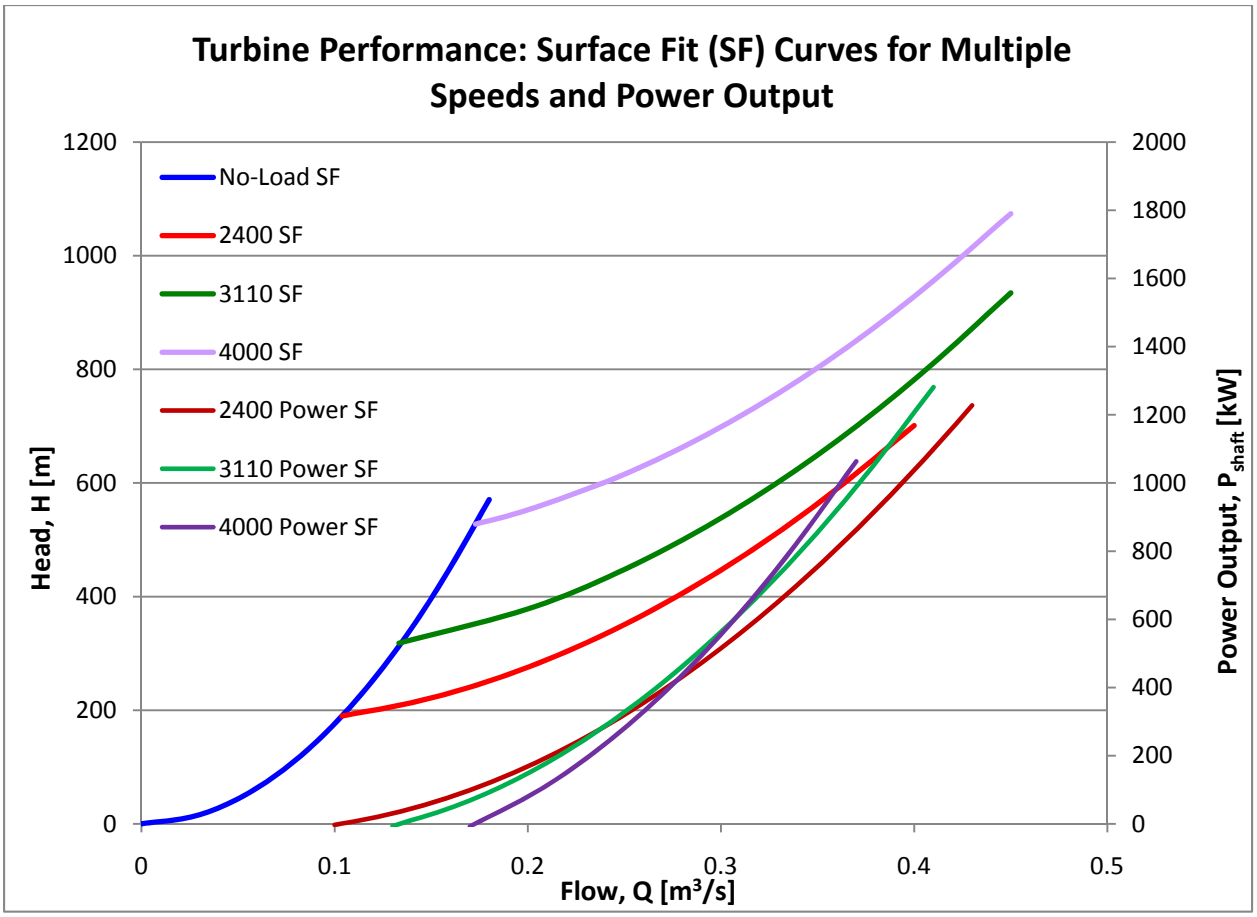

Fig. 3: Shaft Power Surface Fit Curves with Turbine Performance

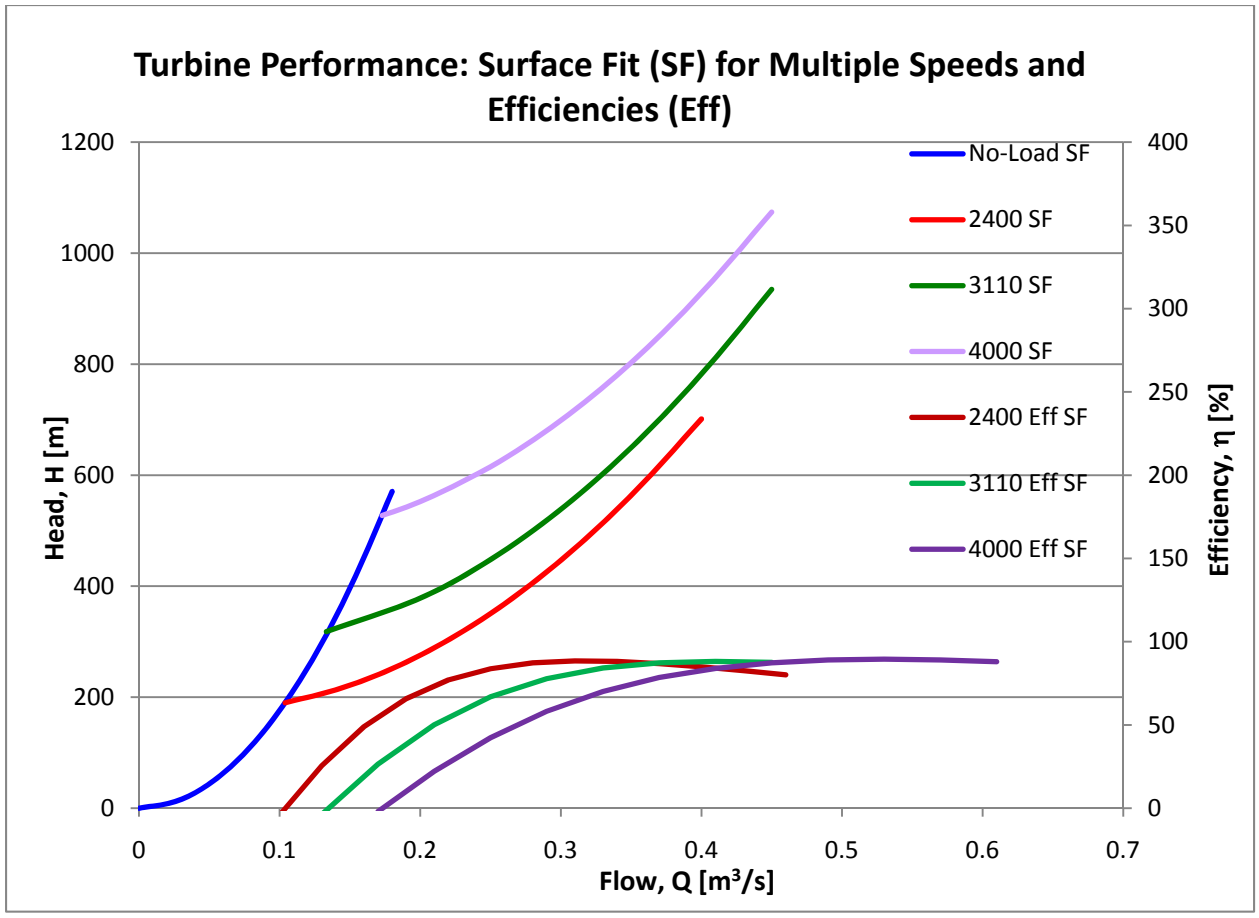

Fig. 4: Efficiency

Best Efficiency

The BEP corresponds to the flow and head at the maximum on the efficiency curve. To find the efficiency curve maximum, the first derivative of Eq. 17 with respect to Q is set equal to zero. It is found that the maximum efficiency flow rate, Q_{BEP}, is a function of all of the surface fit constants and the rotational speed,

$$Q_{BEP} = N_{BEP}\lambda\left[1 + \sqrt{1 + \xi}\right] \tag{18}$$

Where, ξ is the BEP Constant and is defined as,

$$\xi = \frac{\beta + \gamma\lambda}{\alpha\lambda^2} \tag{19}$$

The BEP Constant signifies a very important relationship between the BEP and recirculation flow. If the value of ξ is greater than zero, γ is greater than the ratio of β/λ and the turbine functions as desired. However, if the value of ξ is less than zero, then γ

is less than the ratio β/λ and recirculation flow becomes a dominant factor in the turbine operation, resulting in undesired performance.

Figure 5 is a plot showing the results of the above generated efficiency and BEP equations and resulting values for 2400 RPM and 3110 RPM specifically.

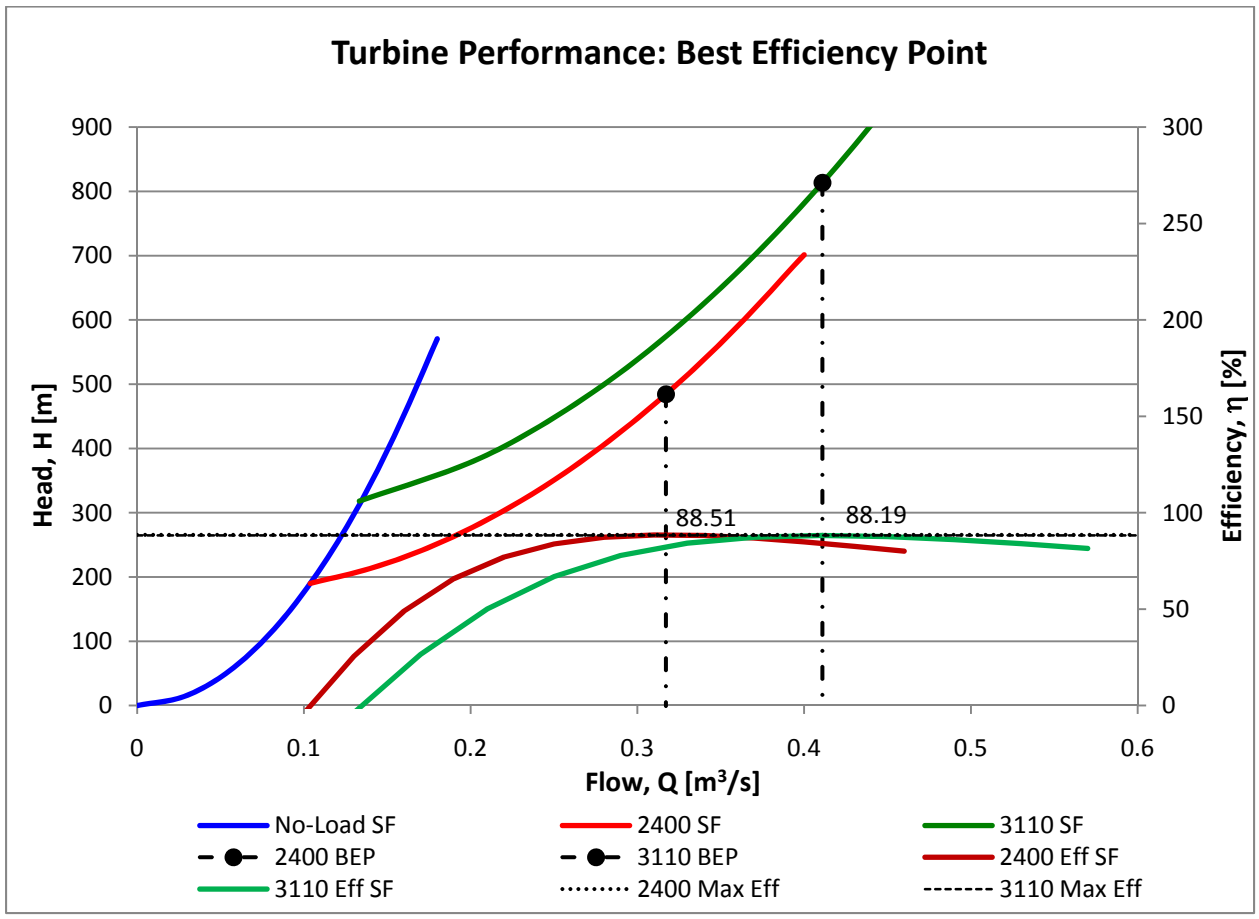

Fig. 5: BEP

Figure 5 shows that the tangent lines to the maximum efficiency curves are practically on top of each other and that the difference between the two maximum efficiencies is 0.32%. This confirms that at any flow rate, or head the rotational speed can be adjusted to maintain maximum efficiency.

Conclusions

The equations and results shown above provide complete liquefied gas reaction turbine performance in the most general form and based upon major principals including, conservation of energy, conservation of momentum, and the affinity law relationships.

Typically, older models used to define turbine efficiency have proven to be good a basis, but are generally accepted as somewhat inaccurate. The presented efficiency

equation based on the developed hydraulic power and actual power equations represent, and more accurately model, actual turbine performance and efficiency. Thus, providing a better representation of performance overall.

The discovered BEP Constant provides important insight into turbine performance and the recirculation flow. Future turbine design will benefit from investigating and understanding this relationship.

It is also important to note that the speed curves are not evenly spaced and tend to curve up towards the next speed as flow increases (Fig. 2 – Fig. 5). This has been experienced in actual test data, but was not sufficiency accounted for by previous performance models. The General Performance Equation (Eq. 1a) models this observed result through the third term, γQN, which represents the recirculation that occurs within the hydraulics (Alison-Youel, 2008). It can be further concluded that the performance envelope created by the no-load and locked-rotor curves as developed by Finley (2008) will encompass the experienced, and now more accurately modeled speed curves.

The general hydraulic and shaft power equations coupled with the developed efficiency and BEP relationships presented in this paper, more accurately model actual liquefied gas reaction turbine performance. These and those presented by Finley (2008) represent a movement towards further turbine performance understanding and the capability to more accurately model performance in a simple and well supported manner.

References

Alison-Youel, S.D. "Observation and analysis of affinity law deviations through tested performance of liquefied gas reaction turbines." International Journal of Rotating Machinery (IJRM), Vol. 2008. Article ID 737285.

Cengel, Y.A., Boles, M. A. Thermodynamics: An Engineering Approach (4th Ed.). McGraw Hill, 2002.

Courant, R., Fritz, J. Introduction to Calculus and Analysis. Springer, 2000.

Finley, C.D. “Comparing predicted and tested performance of cryogenic reaction turbines under locked-rotor condition.” 12th International Symposium on Transport Phenomena and Dynamics of Rotating Machinery (ISROMAC). Honolulu, Hawaii, February 17-22, 2008. ISROMAC12-2008-20252.

Kimmel, H. E. “Speed Controlled Turbines for power recovery in cryogenic and chemical processing.” World Pumps, June 1997.

Lobanoff, V.S., Ross, R.R. Centrifugal Pumps, Design and Application. Gulf Publishing, 1992.

Biography of Speaker

Sarah Alison-Youel received a Bachelor of Science degree in Mechanical Engineering with a minor in Mathematics from the University of Nevada, Reno in 2006. Since joining Ebara in 2007 she has been working with prototype engineering, taking a project from concept through to final testing. Currently Sarah is the Project Engineer for the first two-phase Tandem Expander™, two of which will be installed in a Polish Oil and Gas LNG plant in Poland. Sarah has several research papers published in the American Institute of Chemical Engineers and the International Symposium on Transport Phenomena and Dynamics of Rotating Machinery conference proceedings. In addition, a research paper has been published in the International Journal of Rotating Machinery. salison-youel@ebaraintl.com